MRS Communications (2018), *8*, 1050–1057

doi:10.1557/mrc.2018.140

MRS Communications

Research Letter

Ultra-low Pt-decorated NiCu bimetallic alloys nanoparticles supported on reduced graphene oxide for electro-oxidation of methanol

Ammar Bin Yousaf*, Sajeda Adnan Mutlaq Alsaydeh, Fathima Sifani Zavahir, Peter Kasak, and **Syed Javaid Zaidi*,** Center for Advanced Materials, Qatar University, Doha 2713, Qatar

*Address all correspondence to Yousaf and Zaidi at **ammar.chemist18@gmail.com**, **ammar@mail.ustc.edu.cn**, **muhammad.ammar@qu.edu.qa** and **szaidi@qu.edu.qa**

(Received 25 May 2018; accepted 13 July 2018)

Abstract

The selectivity of catalyst is an essential factor in direct methanol fuel cells (DMFCs) and plays an important role to improve their performance. To this end, platinum (Pt)-based low-cost trimetallic catalysts have been developed. The catalyst comprising ultra-low Pt-decorated NiCu bimetallic alloys nanoparticles fabricated on reduced graphene oxide (rGO). The series of Pt-NiCu/rGO nanocomposites were synthesized with different compositions to obtain the optimal conditioned material. The electrochemical results showed good performance for the electro-oxidation of methanol at anodic end of DMFCs. These outcomes opened up a broad avenue for developing lower cost-active catalysts with better performance for DMFCs.

Introduction

Renewable energy devices attracted huge attention to overcome the depletion of fossil fuels and mitigate the faced energy challenges for present and upcoming human societies. Among those, direct methanol fuel cells (DMFCs) are one of them to produce clean energy with environmentally safe nature. Plenty of work had been done to improve the DMFCs anodes for achieving enhanced and durable performance.[1,2] The platinum (Pt) or Pt-based catalysts were extensively used as anode materials for electro-oxidation of methanol in DMFCs.[3] Later on, due to the poisoning and degradation issues of monometallic Pt, other noble metals were incorporated with Pt to develop bimetallic or trimetallic electrocatalysts with enhanced performance.[4,5] These strategies also faced challenges, as the catalysts cannot balance the overall cost of DMFCs at industrial levels, where the reason is that the high cost and the low-abundant noble metals are unable to resolve these problems.[6] In particular, the past research also proved that the dispersion of active catalysts on conductive support materials is also important to obtain maximum performance of the whole catalyst materials, such as on carbon black, carbon nanotubes, and reduced graphene oxide (rGO). Hence, the rGO can be widely used as a promising candidate among them, to fabricate the metallic catalysts in DMFCs, due to its unique properties, i.e., the enhanced mechanical and electronic properties.[7,8]

Earth-abundant transition metals remained an auspicious choice to use in a combination with precious metals to overcome the cost effects in large-scale industries. In a family of transition metals, nickel (Ni)[9,10] incorporated with other noble and non-noble metals such as Pt, palladium (Pd)[11,12] copper (Cu),[13] manganese[14] as electrocatalysts is considered as a promising approach. These transition metals favorably work for chemisorptions of methanol owing similar behavior related to noble metals. The major concerns for enhanced methanol oxidation reactions (MOR) consist of adsorption of methanol molecules and their conversion into active intermediates, simultaneous dissociation of water molecules to mitigate the carbon monoxide (CO) poisoning issue during MOR.[11–12] The elements like Cu can facilitate the adsorption of methanol molecules similarly as Pt/Pd and their oxidation into active intermediates.[13] Whereas, the presence of Ni can highly promote the Ru- and Pd-like behavior for dissociation of water molecules and produce $–OH_{ads}$ species to react with adjacent $–CO_{ads}$ present at Pt-active sites.[9,10] This so-called bi-functional mechanism can highly enhance the performance of catalysts. Herewith, the faced crucial challenges in DMFCs field have been considered, such as the cost and the performance for developing active anode catalysts. For the very first time, we have introduced a unique nanocomposite-like material with relatively lower cost, enhanced, and durable activity for MOR. The bimetallic alloys of NiCu were synthesized on three-dimensional conductive carbon base rGO support material; afterwards, the ultra-low decoration of Pt nanoparticles (NPs) were drawn on pre-synthesized NiCu/rGO material to develop Pt-NiCu/rGO nanocomposite following wet-chemical method, as anode catalyst for DMFCs.

Experimental

Reagents

$NiCl_2.6H_2O$, $CuCl_2.2H_2O$, cetyltrimethylammonium bromide (CTAB), sodium borohydride ($NaBH_4$), H_2PtCl_6, ascorbic

acid, CH_3OH (99.9%) was purchased from J.T. Baker, and potassium hydroxide (KOH). All reagents were of analytical-reagent grade.

Characterizations

The crystallographic structure, morphology, and element compositions of the synthesized catalyst were studied by scanning electron microscopy (SEM), x-ray diffraction (XRD), FTIR, thermal gravimetric analysis (TGA), and x-ray photoelectron spectroscopy (XPS). The XRD patterns of the samples were collected on a Rigaku/Max-3A x-ray diffractometer with Cu K_α radiation (λ = 1.54178 Å); the operation voltage and current were maintained at 40 kV and 200 mA, respectively. The XPS was performed at a Perkin-Elmer RBD upgraded PHI-5000C ESCA system.

Synthesis procedure for NiCu/rGO bimetallic alloys

In the first step, disperse 0.5 mL of graphene oxide solution in 2 mL of distilled water or Mili-Q water. Dissolve 0.237 g of $NiCl_2.6H_2O$ and 0.170 g of $CuCl_2.2H_2O$ in 2.5 mL of distilled water or Mili-Q water. Mix both the above solutions together with continuous stirring and then add 0.1 g of CTAB in this solution. After some time, add $NaBH_4$ (0.010 g of $NaBH_4$ in 1.5 mL water). With continuous stirring of solution as the color of solution turns black, stop the reaction. Then centrifuge the solution mixture and wash the residue with water and ethanol three times. After washing, place the residue in vacuumed oven for drying at 60°C.

Synthesis procedure for Pt-NiCu/rGO bimetallic alloys

In the second step, disperse 0.5 mg of pre-synthesized NiCu/rGO in 2 mL of distilled water or Mili-Q water. Then add 0.5 mL of 10 mM H_2PtCl_6 in it, then mix the above solution with continuous stirring and heat it up to 80°C then add 80 µL of ascorbic acid with continuous stirring and heating for 30 min. Then centrifuge the solution mixture and wash the residue with water and ethanol three times. After washing, place the residue in vacuumed oven for drying at 60°C.

Electrochemical measurements

Before each electrochemical experiment, a glassy carbon electrode (0.196 cm^2 geometric surface are) was first polished with alumina slurries (Al_2O_3, 0.05 mm) on a polishing cloth to obtain a mirror finish, followed by sonication in 0.1 M HNO_3, 0.1 MH_2SO_4, and pure water for 10 min, successively. To prepare a catalyst supported working electrode, 10 µL of 2 mg/mL suspension in ethanol was drop-coated on the polished electrode surface by a micro liter syringe, with a catalyst loading of 0.1 mg/cm^2, followed by drying in vacuum at room temperature. Afterwards, the catalyst was covered with a thin layer of Nafion (0.1 wt.% in water, 5 µL) to ensure that the catalyst was tightly attached to the electrode surface during the electrochemical measurements. Voltammetry measurements were carried out with a Gamry electrochemical workstation. The electrode prepared above was used as the working electrode. The Ag/AgCl (in 3 M KCl, aq.) combination, isolated in a double junction chamber, and a Pt coil were used as the reference and counter electrodes, respectively. All the measurements were performed in electrochemical experiments with respect to the standard values of reversible hydrogen electrode. Electrochemical experimental work was done by potential cycling methods for MOR studies in 0.1 M KOH + 1 M CH_3OH solution with N_2 purging at a scan rate of 50 mV/s[1].

Results and discussion

A combined wet-chemical and dry chemistry method have been adopted to develop a highly efficient and active catalyst for electro-oxidation of methanol in DMFCs. In the first step of synthesis, CTAB capping agent was used to control the size and spherical geometry of as-synthesized composite material on the surface of rGO support. Bimetallic alloys of earth-abundant metals, NiCu, were successfully incorporated on rGO following the ultra-low fabrication of Pt NPs on NiCu alloys in the second step via wet-chemical method. As it is also documented that the capping agent is not favorable for electrocatalytic performance of materials, in order to remove the CTAB from catalyst surface, the Pt-NiCu/rGO catalysts were experienced through pyrolysis at about 250°C. In the present work, the series of electrocatalysts was synthesized and atomic composition among NiCu bimetallic alloys was tuned and presented as Ni_1Cu_3, Ni_1Cu_1, and Ni_3Cu_1; afterwards, the equal ultra-low loadings of 2 wt.% of Pt was fabricated on all these catalysts, forming the finally presented Pt-Ni_1Cu_3/rGO, Pt-Ni_1Cu_1/rGO, and Pt-Ni_3Cu_1/rGO nanocomposites. The real Ni, Cu, and Pt loadings in all Pt-NiCu/rGO catalysts were also analyzed by ICP-MS analysis to evaluate the difference between actual and nominal metal loadings. Whereas, the actual loadings are evaluated by ICP-MS analysis and the nominal loadings represent the values assumed and were used during the synthesis of catalysts. These measurements also confirm the 1:3, 1:1, and 3:1 compositions of Ni:Cu, respectively, in all the catalysts. The detailed Ni, Cu, and Pt molar and weight percentage (wt.%) measurements for all the catalysts are provided in Table S1. The aim of the present work was mainly focused on the synthesis of highly active, durable, and lower cost material as anode catalyst for DMFCs. In line with the aim, we only tuned the compositions of cheap transition metals to obtain the maximum performance of catalyst and decorated with a fixed amount of 2 wt.% Pt NPs. Whereas, the ultra-low loadings of Pt in the present work can be defined as, in the previous studies the fuel cells electrocatalysts have been developed up to 20 wt.%.[15–16] Herein, we have been successful for developing an electrocatalyst for DMFCs with nearly roughly comparable enhanced performance of catalysts in the literature.[17]

The SEM was implied for morphology and structural analysis of the above synthesized nanocomposite materials, shown in Fig. 1(a). The SEM images show sucessful synthesis of nanocomposites on the surface of rGO; the spots of these

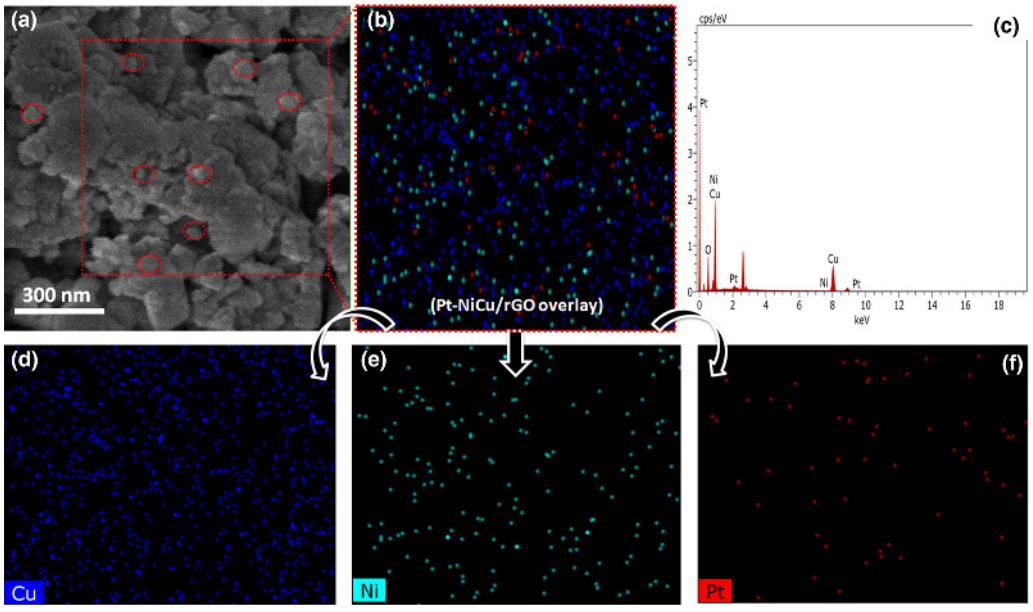

Figure 1. (a) SEM image of Pt-Ni_1Cu_3/rGO catalyst with red-dotted circles representing Pt-Ni_1Cu_3 nanocomposites on the surface of rGO. (b) Overlay image of elemental mapping of all the elements included in Pt-Ni_1Cu_3/rGO catalyst for the selected area of SEM micrograph. (c) EDX spectrum with signatures of all the elements included in Pt-Ni_1Cu_3/rGO catalyst for the selected area of SEM micrograph. (d–f) Individual images of elemental mapping of all the elements, such as Cu, Ni, and Pt, respectively, included in Pt-Ni_1Cu_3/rGO catalyst.

nanocomposites encircled with red-dotted lines in the figure to show their presence. The disperssion of each metal inside the nanocomposite material was further investigated by elemental mapping characterizations. As shown in Fig. 1(b), the overlay pattern of selected area element mapping [from Fig. 1(a)] all the elements such as Ni, Cu, and Pt spots is uniformly intermixed to constitute the composite structure. The energy-dispersive x-ray (EDX) result of corresponding elemental mapping area showed visible signatures of each contributing element, as shown in Fig. 1(c). The individual element mapping micrograph of highly active electrocatalyst strongly supporting the stated claim that Cu is in higher proportions than that of Ni in Pt-Ni_1Cu_3/rGO catalyst [see Figs 1(d) and 1(e)], whereas, the ultra-low Pt loadings are also strongly defended by rare Pt spots shown in Pt elemental mapping micrograph [see Fig. 1(f)]. Furthermore, the uniform dispersion of individual element inside nanocomposite exhibited by element mapping is also giving the proof of intimate contact of as-synthesized nanocomposite onto rGO support material.

The crystalline structural testing of prepared nanocomposites was carried out by XRD patterns. Figure 2(a) shows the characteristic reflections of Pt peaks of a polycrystalline face-centered cubic (fcc) structure indexed to Pt (JCPDS, card no 04-0802) along with[18] fcc crystalline Ni corresponds to the planes (111), (200), and (220) at 2θ values of about 44.048°, 51.319°, and 75.683° respectively, intermixed with Cu peaks at the roughly nearly regions as in-line with the literature.[11] The slight shift in the diffraction peaks designated for Cu indicates that the Ni particles have incorporated into the Cu lattice resulting the formation of an alloy between Ni and Cu.[19] As shown in Fig. 2(a), the characteristic peaks of Cu (111) are negatively shifting toward lower θ values and Cu (220) are shifting toward Ni (220) forming the bimetallic geometries. These shifts in peaks are also presented with dotted lines inside the XRD spectra, where the shifting of peaks can be ascribed by peak intensities and as well the location of peaks.[20,21] The XRD patterns also show the characteristic peaks of (002) planes of the graphite-like structure at $2\theta = 25.374°$ that came from rGO support material.[22,23] To compare the apparent difference in XRD pattern before and after the decoration of Pt entities, the XRD results for NiCu alloys with and without Pt NPs are shown in Fig. 2(b). These results are clearly showing the reduction of Pt NPs on NiCu alloys along with the fcc lattice of these alloys forming a composite material consisting of three elements sharing the lattice.

FTIR analysis was performed to investigate and confirm the reduction of oxygenated/oxygen-containing groups on the surface of GO after the fabrication of metallic nanocomposite on its surface; these fabrications of Pt-NiCu on GO also lead to its reduction into rGO. Figure 2(c) shows a typical FTIR behavior of the whole prepared series of Pt-NiCu catalysts on rGO. Whereas, the precise analysis of oxygenated groups reduction could be seen in Fig. 2(d); these results provide information about the effective reduction of GO in to rGO after the incorporation of nanocomposites on graphene oxide surface leading to the synthesis of Pt-NiCu/rGO. The two peaks with intensity at 1734 and 1050/cm correspond to the C=O and C–O–C bonds, which are reduced for Pt-Ni_1Cu_3/rGO catalyst. Similarly, the

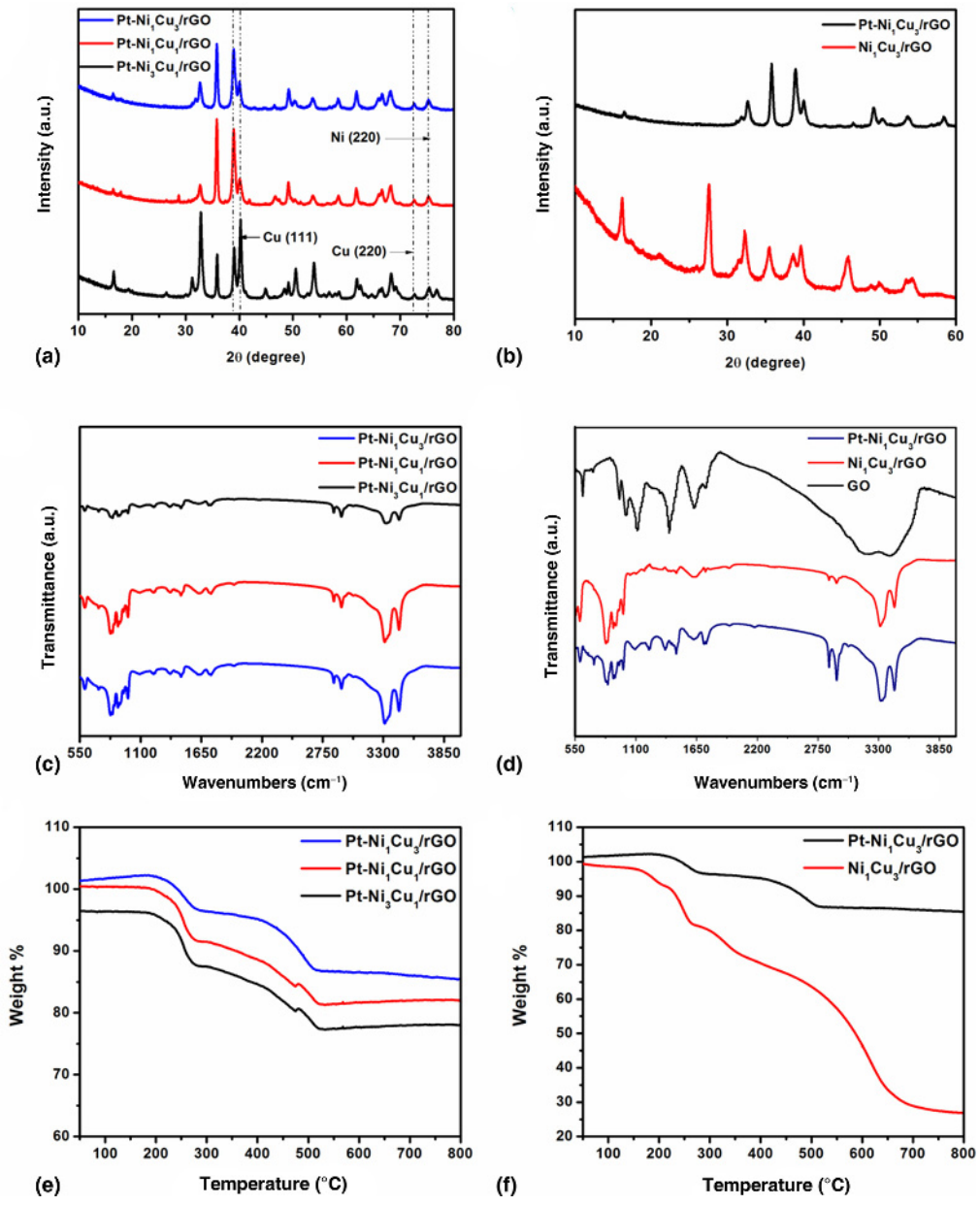

Figure 2 (a) XRD spectra of all the prepared catalysts in a series, (b) XRD spectra of Pt-Ni_1Cu_3/rGO in comparison with Ni_1Cu_3/rGO, (c) FTIR spectra of all the prepared catalysts in a series, (d) XRD spectra of Pt-Ni_1Cu_3/rGO in comparison with Ni_1Cu_3/rGO and GO, (e) TGA curves of all the prepared catalysts in a series, and (f) TGA curves of Pt-Ni_1Cu_3/rGO in comparison with Ni_1Cu_3/rGO.

broad peak at about 3300/cm correspond to –OH, predicting to be vanished as after Pt-NiCu fabrication on GO and showing the as-required reduction of GO into rGO at the sites with an intimate supported nanocomposites onto them. TGA was also performed under air atmosphere for all the catalyst materials and also compared with the TGA behavior before and after the Pt NPs fabrication on NiCu alloys for more confirmation about incorporation of nanocomposite material and decoration of Pt NPs with NiCu alloys in a Pt-Ni_1Cu_3/rGO catalyst. The TGA trends are presented in Fig. 2(e), showing the consistent weight loss in a linear relation for the whole series of Pt-NiCu/rGO materials. In contrast, the weight loss behavior is visibly very different between NiCu/rGO and Pt-NiCu/rGO due to the presence of Pt NPs on NiCu surface; the successfully reduced Pt NPs on bimetallic NiCu alloys surface made them stable and heat resistant up to an extent of 500°C, afterwards, stabilizing the nanocomposite material via protecting the outer surface of nanocomposites [see Fig. 2(f)].

The XPS analysis was also done to confirm the reduction of metallic species such as Pt, Cu, and Ni in the nanocomposite

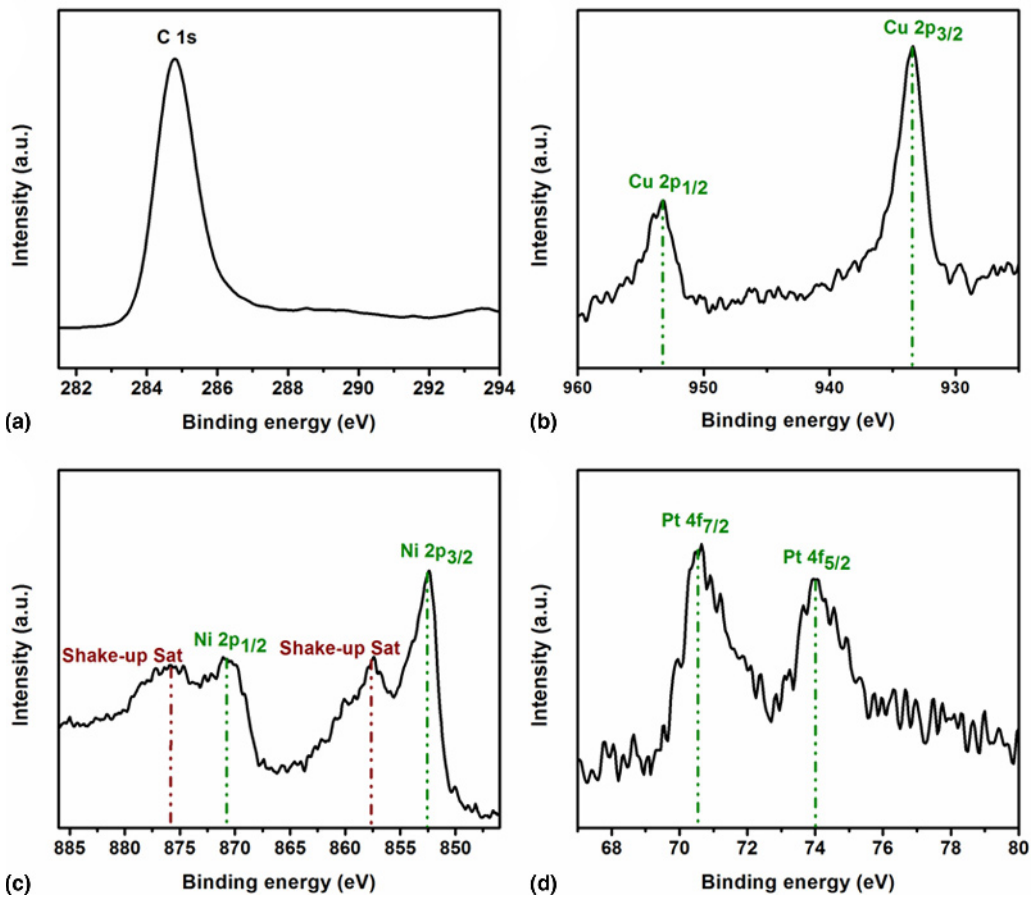

Figure 3. XPS analysis of Pt-Ni_1Cu_3/rGO catalyst, (a) high-resolution C1*s* spectrum of carbon, (b) high-resolution Cu2*p* spectrum of copper, (c) high-resolution Ni2*p* spectrum of nickel, and (d) high-resolution Pt4*f* spectrum of copper platinum.

and also to investigate the characteristic surface oxidations. In addition, the presence of rGO as support material was also strongly verified by XPS spectra of high-resolution C1*s* scan [see Fig. 3(a)]. The C1*s* scan displaying a major peak domain at about 284.7 eV correspond to the C–C groups, showing that C–C groups are dominated over other minor proportions of domains nearly about 286.1 and 288.0 eV, which correspond to C–O and C=O functionalities. These results verified the presence of rGO in Pt-Ni_1Cu_3/rGO catalyst.[24] The signatory peaks of Cu were found at 934.18 and 953.36 eV, whereas the broadening of these region indicates the presence of Cu^{1+} and Cu^{2+}, and the presence of higher proportion peak area ascribed to Cu^{2+} coinciding mainly at 934.18 and 953.36 eV is a further evidence on forming Cu^{2+} in nanocomposite material [see Fig. 3(b)].[25] The split orbit peaks of Ni $2p_{3/2}$ and Ni $2p_{1/2}$ at 853.80 and 870.66 eV, respectively, were formed in a mixed form on the surface of catalyst. Whereas, the presence of satellite shakeup peaks indicates the two oxidation states of Ni, such as Ni^0 and Ni^{2+}, existing [see Fig. 3(c)].[26] However, the Pt 4*f* high-resolution spectrum consists two major domains related to $4f_{5/2}$ and $4f_{7/2}$ with corresponding binding energies of 74.6 and 71.8 eV, respectively, with an asymmetric nature. This XPS behavior revealed the metallic Pt^0 oxidation state of Pt, in the form of Pt NPs decorated on NiCu alloys in a composite material [see Fig. 3(d)].[18]

The electrocatalytic anodic behavior for DMFCs of all the prepared materials was carried out by electro-oxidation of methanol in basic medium by potential cycling method. The CV curves for MOR suggest oxidation of methanol by all the catalysts. In order to isolate the obtained current from methanol oxidation, the cyclic voltammogram was also taken in the absence of methanol in the same base medium and protocol. As the composition of ultra-low Pt remained same in all the catalysts to control the cost of material and NiCu compositions were tuned to get optimal performance catalyst, hence, obtained current from methanol electro-oxidation was expressed in terms of current densities derived from geometric surface areas. The role of Pt interactions with different compositions of NiCu was also expressed by presenting mass activities via current densities derived from mass loadings of Pt for all the catalysts.

As shown in Figs 4(a)–4(c), the oxidation of methanol happened with two characteristic anodic peaks at about after −0.40

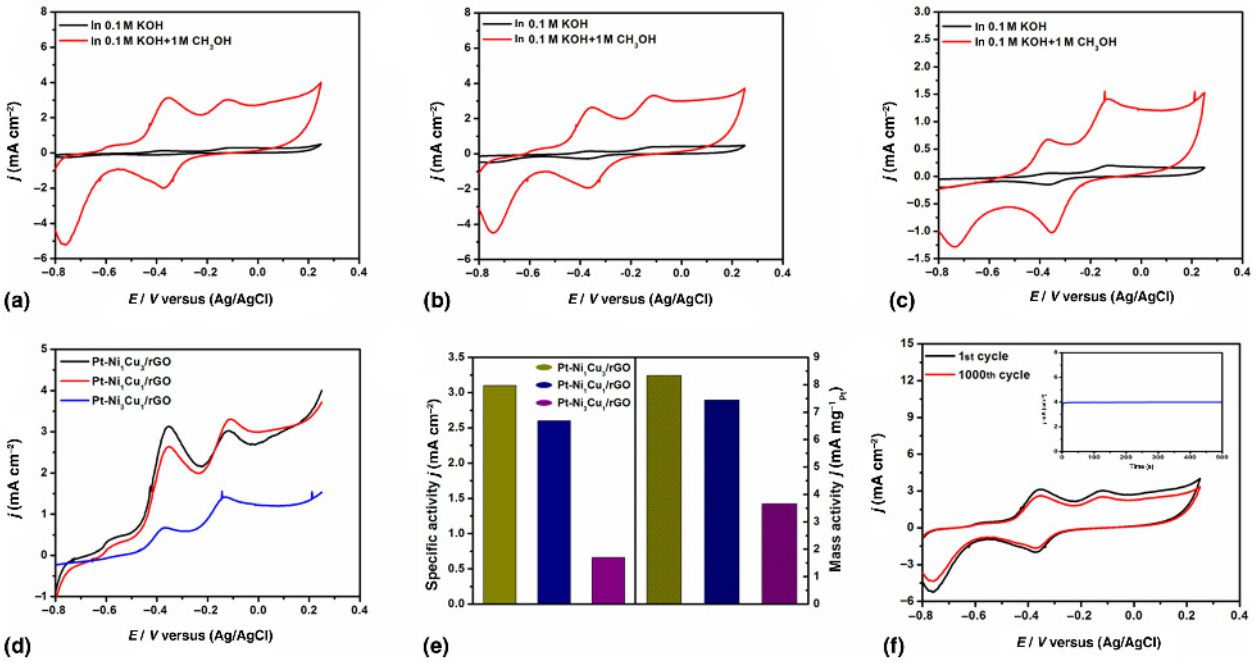

Figure 4. Electrochemical CV results taken in the presence and absence of methanol in 0.1 M KOH and 0.1 M KOH + 1 M CH_3OH, respectively, for the analysis of electrocatalytic MOR performance of (a) Pt-Ni_1Cu_3/rGO catalyst, (b) Pt-Ni_1Cu_1/rGO catalyst, (c) Pt-Ni_3Cu_1/rGO catalyst, (d) onset potential of electrocatalytic MOR curves for all the prepared catalysts, (e) peak current density in terms of both specific activities and mass activities for all the prepared catalysts, (f) accelerated durability test results for Pt-Ni_1Cu_3/rGO catalyst with first and 1000th cycle of MOR activities. **Inset:** The chronoamperometry results for Pt-Ni_1Cu_3/rGO catalyst in the same environment and medium at a constant potential of −0.45 V versus Ag/AgCl also exhibit the long-time stability in the obtained current value.

and −0.25 V. According to the chemistry of present materials, the first peak ascribed mainly to the methanol electro-oxidation. Herein, the methanol molecules are adsorbed on the surface of active Pt and Cu alliance sites,[27] whereas, the simultaneous dissociation of water molecules proceeded on nearby Ni sites. This phenomenon processed the oxidation of methanol at lower potential values to produce the final product CO_2.[28] Afterwards, the second MOR peak may ascribe with the phenomenon, i.e., the Pt-active sites also become blocked by CO_{ads} species that appeared during MOR. These blocked Pt sites are further unblocked by the presence of adjacent OH_{ads} species produced during dissociation of water molecules. The reactions between CO_{ads} and OH_{ads} produce the final product CO_2 within MOR electrocatalysis.[28,29]

The performance of methanol oxidation electrocatalysts can be screened out by two major factors, such as onset potential and current densities. Therefore, we have presented a precise analysis of MOR activities by both of these parameters. The onset potential of MOR significantly moved to the lower potential values in case of Pt-Ni_1Cu_3/rGO [see Fig. 4(d)]. Similarly, the current density values showed increasing trends as Pt-Ni_3Cu_1/rGO<Pt-Ni_1Cu_1/rGO<Pt-Ni_1Cu_3/rGO [see Fig. 4(e)]. These can be explained as, in bimetallic alloys of NiCu, Cu is mainly considered to be taking part in the oxidation of methanol molecules as an alliance form along with both Pt and Ni and it can also adsorb methanol molecules for their chemisorptions. Whereas, Ni is associated with dual factors, i.e. methanol chemisorptions and dissociation of water molecules.[27,19] Therefore, decreasing the composition of Ni in bimetallic alloys positively enhanced methanol electro-oxidation. The strong Pt and Cu interactions mainly adsorb the methanol molecules and their intermediate species on their active sites for getting quick and higher oxidation of methanol following the so-called bi-functional mechanism.[28] The low-content of Pt compensated by the presence of higher proportion of Cu and highly conductive rGO support lead to smooth six electrons transfer phenomenon for successful methanol oxidation. Moreover, the comparison of methanol electro-oxidation with a without Pt loading has also been derived and the results proved enhanced performance of NiCu bimetallic alloys after low-content decoration of Pt NPs in association with both the metals (see Fig. S1).

The durable nature of an electrocatalyst is another important and key parameter for their applications in practical fuel cells. Herewith, to evaluate the durability of catalyst, accelerated durability tests (ADTs) was also run in the same medium and environment for MOR, by applying a cyclic potential sweep at a scan rate of 100 mV/s up to 1000 cycles. The catalyst Pt-Ni_1Cu_3/rGO with higher activity experienced a loss of approximately 1.2% with respect to its highest current density values after 1000 cycles [see Fig. 4(f)]. This ADTs result along with electrocatalytic MOR suggests enhanced and

durable performance of Pt-Ni_1Cu_3/rGO catalyst for its practical applications in DMFCs at the anodic end. Moreover, the stability and durability in the obtained current value were also tested by chronoamperometry analysis at a constant potential value. The obtained current has shown stability in its nature and has shown superior performance than already reported results with higher loadings of Pt in methanol electro-oxidation catalysts.[16,28,30] Hence, enhanced and durable MOR activities attributed to the mutual presence and electrons transference among NiCu alloys with low-content Pt NPs dispersed on rGO support constituting overall low-cost anode catalyst for DMFCs.

Conclusions

In conclusions, for the first time, we have developed relatively active and economically low-cost anode catalysts for the applications of DMFCs. Earth-abundant elements with superior electrocatalytic behavior replaced un-abundant or precious metals with satisfactory performances. Lower cost NiCu bimetallic alloys with tuned compositions were successfully synthesized, leading to the decoration of low-content Pt NPs on NiCu bimetallic alloys. These Pt-NiCu nanocomposites were highly dispersed on the surface of rGO and characterized by means of several important physical characterizations to confirm the successful synthesis of as-designed materials. The characteristic results from structural and crystallite analysis revealed intimate contact among elements in nanocomposite material and as well with conductive support. These features strongly favor the mutual transference of electrons from support to the nanocomposite and among the composite members to facilitate enhanced electrocatalysis on their surfaces. The prepared catalyst materials were tested for the electro-oxidation of methanol in basic medium and shown highly active and durable performance for MOR. These facile strategies may open up green routes for developing lower cost electrocatalysts materials and can replace or minimize the consumption of un-abundant or precious metals with alternative earth-abundant elements in the field of renewable and sustainable energy applications.

Acknowledgments

The authors acknowledge financial support from the Qatar National Research Fund (A Member of The Qatar Foundation) NPRP grant #9-219-2-105. The statements made herein are solely the responsibility of the authors.

Supplementary Material

The supplementary material for this article can be found at https://doi.org/10.1557/mrc.2018.140

References

1. O. Winjobi, Z. Zhang, C. Liang, and W. Li: Carbon nanotube supported platinum–palladium nanoparticles for formic acid oxidation. *Electrochim. Acta* **55**, 4217 (2010).
2. E. Antolini and E.R. Gonzalez: Alkaline direct alcohol fuel cells. *J. Power Sources* **195**, 3431 (2010).
3. A.B. Yousaf, M. Imran, N. Uwitonze, A. Zeb, S.J. Zaidi, T.M. Ansari, G. Yasmeen, and S. Manzoor: Enhanced electrocatalytic performance of Pt_3Pd_1 alloys supported on CeO_2/C for methanol oxidation and oxygen reduction reactions. *J. Phys. Chem. C* **121**, 2069 (2017).
4. M.K. Debe: Electrocatalyst approaches and challenges for automotive fuel cells. *Nature* **486**, 43 (2012).
5. S.J. Zaidi, M. Bello, A. Al-Ahmed, A.B. Yousaf, and M. Imran: Mesoporous carbon supported Pt/MO_2 (M=Ce, Pr, Nd, Sm) heteronanostructure: promising non-Ru methanol oxidation reaction catalysts for direct methanol fuel cell application. *J. Electroanal. Chem.* **794**, 86 (2017).
6. J. Wu and H. Yang: Platinum-based oxygen reduction electrocatalysts. *Acc. Chem. Res.* **46**, 1848 (2013).
7. Y. Huang, H. Huang, Q. Gao, C. Gan, Y. Liu, and Y. Fang: Electroless synthesis of two-dimensional sandwich-like Pt/Mn_3O_4/reduced-graphene-oxide nanocomposites with enhanced electrochemical performance for methanol oxidation. *Electrochim. Acta* **149**, 34 (2014).
8. J. Liu, Z. Liu, C.J. Barrow, and W. Yang: Molecularly engineered graphene surfaces for sensing applications: a review. *Anal. Chim. Acta* **859**, 1 (2015).
9. R. Ojani, J.-B. Raoof, S. Fathi, and S. Alami-Valikchali: Electrochemical behavior of Ni (II) incorporated in zeolite Y-modified carbon electrode: application for electrocatalytic oxidation of methanol in alkaline solution. *J. Solid State Electrochem.* **15**, 1935 (2011).
10. M. Risbud, S. Baxter, and M. Skyllas-Kazacos: Preparation of nickel modified carbon fibre electrodes and their application for methanol oxidation. *Open Energy Fuels J.* **5**, 9 (2012).
11. Y. Zhao, X. Yang, J. Tian, F. Wang, and L. Zhan: Methanol electrooxidation on Ni@ Pd core-shell nanoparticles supported on multi-walled carbon nanotubes in alkaline media. *Int. J. Hydrogen Energy* **35**, 3249 (2010).
12. R. Amin, R.A. Hameed, K. El-Khatib, and M.E. Youssef: Electrocatalytic activity of nanostructured Ni and Pd–Ni on Vulcan XC-72R carbon black for methanol oxidation in alkaline medium. *Int. J. Hydrogen Energy* **39**, 2026 (2014).
13. I. Danaee, M. Jafarian, F. Forouzandeh, F. Gobal, and M. Mahjani: Electrocatalytic oxidation of methanol on Ni and NiCu alloy modified glassy carbon electrode. *Int. J. Hydrogen Energy* **33**, 4367 (2008).
14. R. Tammam, A. Fekry, and M. Saleh: Electrocatalytic oxidation of methanol on ordered binary catalyst of manganese and nickel oxide nanoparticles. *Int. J. Hydrogen Energy* **40**, 275 (2015).
15. I. Katsounaros, J.C. Meier, and K.J.J. Mayrhofer: The impact of chloride ions and the catalyst loading on the reduction of H_2O_2 on high surface area platinum catalysts. *Electrochim. Acta* **110**, 790–795 (2013).
16. J.Y. Lee, D.H. Kwak, Y.W. Lee, S. Lee, and K.W. Park, Synthesis of cubic PtPd alloy nanoparticles as anode electrocatalysts for methanol and formic acid oxidation reactions. *Phys. Chem. Chem. Phys.* **17**, 8642 (2015).
17. G.P. Keeley, S. Cherevko, and K.J.J. Mayrhofer, The stability challenge on the pathway to low and ultra-low platinum loading for oxygen reduction reaction in fuel cells. *ChemElectroChem* **3**, 51 (2016).
18. A.B. Yousaf, M. Imran, A. Zeb, T. Wen, X. Xie, Y.F. Jiang, C.Z. Yuan, and A.W. Xu: Single phase PtAg bimetallic alloy nanoparticles highly dispersed on reduced graphene oxide for electrocatalytic application of methanol oxidation reaction. *Electrochim. Acta* **197**, 117 (2016).
19. I.G. Casella, M.R. Guascito, and M.G. Sannazzaro: Voltammetric and XPS investigations of nickel hydroxide electrochemically dispersed on gold surface electrodes. *J. Electroanal. Chem.* **462**, 202 (1999).
20. D. Li, P. Lv, J. Zhu, Y. Lu, C. Chen, X. Zhang, and Q. Wei, NiCu alloys nanoparticles-loaded carbon nanofibers for phenolic biosensor applications. *Sensors* **15**, 29419 (2015).
21. B. Zhao, G. Shao, B. Fan, W. Zhao, and R. Zhang, Preparation and electromagnetic waves absorption properties of novel dendrite-like NiCu alloys composite. *RSC Adv.* **5**, 42587 (2015).
22. J. Prabhuram, T. Zhao, Z. Tang, R. Chen, and Z. Liang: Multiwalled carbon nanotube supported PtRu for the anode of direct methanol fuel cells. *J. Phys. Chem. B* **110**, 5245 (2006).
23. G. Guo, F. Qin, D. Yang, C. Wang, H. Xu, and S. Yang: Synthesis of platinum nanoparticles supported on poly (acrylic acid) grafted MWNTs and their hydrogenation of citral. *Chem. Mater.* **20**, 2291 (2008).

24. S. Temiz, Z. Mutlu, S. Shahrezaei, M. Ozkan, and C.S. Ozkan: Effect of intermittent oxygen exposure on chemical vapor deposition of graphene. *MRS Commun.* **7**, 826 (2017).
25. H.H. Hsieh, Y.K. Chang, W.F. Pong, J.Y. Pieh, P.K. Tseng, T.K. Sham, I. Coulthard, S.J. Naftel, J.F. Lee, S.C. Chung, and K.L. Tsang: The electronic structure of Ni-Cu alloys: d-electron charge distribution. *Phys. Rev. B* **57**, 15204 (1998).
26. Q. Guo, D. Liu, X. Zhang, L. Li, H. Hou, O. Niwa, and T. You: Pd–Ni alloy nanoparticle/carbon nanofiber composites: preparation, structure, and superior electrocatalytic properties for sugar analysis. *Anal. Chem.* **86**, 5898 (2014).
27. M. Jafarian, R. Moghaddam, M. Mahjani, and F. Gobal: Electro-catalytic oxidation of methanol on a Ni–Cu alloy in alkaline medium. *J. Appl. Electrochem.* **36**, 913 (2006).
28. L.F. Lu, S. Chen, S. Thota, X.D. Wang, Y.C. Wang, S.H. Zou, J. Fan, and J. Zhao: Composition controllable synthesis of PtCu nanodendrites with efficient electrocatalytic activity for methanol oxidation induced by high index surface and electronic interaction. *J. Phys. Chem. C* **121**, 19796 (2017).
29. S. Sharma, A. Ganguly, P. Papakonstantinou, X. Miao, M. Li, J. L. Hutchison, M. Delichatsios, and S. Ukleja: Rapid microwave synthesis of CO tolerant reduced graphene oxide-supported platinum electrocatalysts for oxidation of methanol. *J. Phys. Chem. C* **114**, 19459 (2010).
30. R. Bavand, Q. Wei, G. Zhang, S. Sun, A. Yelon, and E. Sacher, PtRu alloy nanoparticles. 2. Chemical and electrochemical surface characterization for methanol oxidation. *J. Phys. Chem. C* **121**, 23120 (2017).